

## Supporting Information

# Generation of $V_{Br}^{\bullet}V_{Bi}^{'''}V_{O}^{\bullet\bullet}$ Defect Cluster for $^1O_2$ Production in Molecular Oxygen Activation of Photocatalysis

Jie Ding,<sup>†</sup> Zan Dai,<sup>†</sup> Fan Tian,<sup>†</sup> Bo Zhou,<sup>‡</sup> Bin Zhao,<sup>‡</sup> Huiping Zhao,<sup>†</sup> Zhiquan Chen,<sup>‡</sup> Yunling

Liu,<sup>1</sup> Rong Chen<sup>\*,†</sup>

<sup>†</sup> School of Chemistry and Environmental Engineering and Key Laboratory for Green Chemical Process of Ministry of Education, Wuhan Institute of Technology, Xiongchu Avenue, Wuhan, 430073, PR China \*Email: rchenhku@hotmail.com

<sup>‡</sup> Hubei Nuclear Solid Physics Key Laboratory, Department of Physics, Wuhan University, Wuhan 430072, PR China

<sup>1</sup> State Key Laboratory of Inorganic Synthesis and Preparative Chemistry, College of Chemistry, Jilin University, Changchun, 130012, PR China

### **Experimental Section**

**Chemicals.** Bismuth nitrate pentahydrate ( $\text{Bi}(\text{NO}_3)_3 \cdot 5\text{H}_2\text{O}$ , 99%), superoxide dismutase (SOD, 3000 units/mg protein), catalase (3000 units/mg protein), tryptophan (98%), 4-chlorothioanisole (98%), 4-methoxythioanisole (98%), and 2-bromothioanisole (98%) were purchased from Aladdin. Mannitol (99%), sodium bromide (NaBr, 99%), sodium azide ( $\text{NaN}_3$ , 97%), acetonitrile (99.8%), nitroblue tetrazolium (NBT, 99%), 1,3-diphenylisobenzofuran (DPBF, 97%), diphenyl sulfide (99%), thioanisole (99%), dimethyl sulfide (98%), diethyl sulfide (98%) and triphenylphosphine (99%) were purchased from Sinopharm Chemical Reagent Co., Ltd. (Shanghai, China). All the reagents were analytical grade and used directly without further purification.

**Preparation.** In a typical synthesis, 0.485 g (1 mmol)  $\text{Bi}(\text{NO}_3)_3 \cdot 5\text{H}_2\text{O}$  and 0.103 g (1 mmol) NaBr were dissolved into 20 mL mannitol aqueous solution (0.1 mol/L) under stirring. Then the obtained solution was transferred to a Teflon-lined stainless steel autoclave to perform solvothermal treatment at 180 °C for 3 h. After cooling down to room temperature naturally, the solid product was collected by centrifugation and washed with deionized water and ethanol for five times. The sample was finally dried in a vacuum oven for 24 h at 60 °C for further characterization (**BOR-3**). Other samples were also prepared under identical conditions by varying the solvothermal time to 6 h (**BOR-6**), 9 h (**BOR-9**), 12 h (**BOR-12**), 15 h (**BOR-15**) and 18 h (**BOR-18**), respectively. The yield of **BOR-6** and **BOR-12** was calculated to be 91.05% and 91.01%, respectively (see table below).

	<b>BOR-6</b>	<b>BOR-12</b>
<i>Theoretical Output / g</i>	0.3049	
<i>Actual Output / g</i>	0.2776	0.2775
<i>Yield / %</i>	91.05	91.01

**Characterization.** Powder X-ray diffraction (XRD) was carried out on Bruker axS D8 Discover (Cu K = 1.5406 Å) at a scan rate of  $2^\circ \text{min}^{-1}$  in the  $2\theta$  range from 10 to 80°. Transmission electron microscopy (TEM) image was recorded on a Philips Tecnai G2 20 electron microscope, using an accelerating voltage of 200 kV. Samples for TEM analysis were prepared by drying a drop of nanocrystal dispersion in absolute ethanol

on carbon coated copper grids. The atomic-resolution HRTEM images was investigated by aberration-corrected STEM *via* a Nion UltraSTEM (Nion) microscope operating at 200 keV and equipped with a cold-field emission gun, a third-generation C3/C5 aberration corrector. X-ray photoelectron spectra (XPS) were performed on a Thermo Scientific ESCLAB 250Xi. All binding energies were referenced to the C 1s peak (284.6 eV) arising from the adventitious carbon. Room-temperature steady-state and time-resolved prompt fluorescence (PF) and phosphorescence (PH) were detected with a Horiba FLTCSPC fluorescence spectrophotometer. Brunauer-Emmett-Teller (BET) specific surface area was analyzed by nitrogen adsorption in a Micrometrics ASAP 2020 nitrogen adsorption apparatus (USA). All the as-prepared samples were degassed at 150 °C for 4 h prior to nitrogen adsorption measurements. Electron paramagnetic resonance (EPR) measurement was carried out using a Bruker EMX 10/2.7 EPR spectrometer (X-band) equipped dual cavity with modulation and microwave frequencies of 100 kHz and 9.4145 GHz, respectively. The g-factors were determined by the WinEPR program. The determination of reactive oxygen species (ROS) was characterized by using a Bruker EMX plus model spectrometer operating at the X-band frequency (9.4 GHz) at room temperature. Before measurement, the mixture of aqueous suspension of samples (100 μL, 40 mg/L) and TEMP solution (1 mL,  $5 \times 10^{-2}$  mol/L,  $^1\text{O}_2$  trapping agent) or DMPO solution (1 mL,  $5 \times 10^{-2}$  mol/L,  $\bullet\text{O}_2^-$  and  $\bullet\text{OH}$  trapping agent) was illuminated for 30 s. A xenon lamp (500 W) without filter was used as the light source. The ROS production was also determined in the presence of  $\text{NaN}_3$  and SOD under identical conditions, respectively. The photocurrent measurement carried out on a CHI 660E workstation (Shanghai, China) in a standard three-electrode cell, which contained 0.5 M  $\text{Na}_2\text{SO}_4$  aqueous solution with a platinum foil and a saturated calomel electrode as the counter electrode and the reference electrode, respectively. The working electrode was prepared according to the following process: 10 mg as-prepared sample (**BOR-12** and **BOR-18**) was mixed with 0.4 mL DMF and 0.1 mL nafion solution (5%, DuPont) to form homogeneous emulsion. Then 0.2 mL the catalyst emulsion was dropwise coated on a 10 mm × 10 mm indium-tin oxide (ITO) glass electrode. The estimated loading amount of the sample is 1 mg/cm<sup>2</sup>. After drying in room temperature, the as-prepared electrode was further annealed at 150 °C for 4 h in a vacuum oven to remove the resin. Photocurrent responses of the photocatalyst were measured at open-circuit potential upon light on and off, with simulated light irradiation provided by a 500 W Xe lamp.

**Positron Annihilation Measurement.** The positron lifetime spectra were carried out on conventional fast-fast coincidence lifetime spectrometer with a time resolution of 220 ps in full width at half-maximum (FWHM). A  $^{22}\text{Na}$  positron source with the intensity of about 20  $\mu\text{Ci}$  was sandwiched between two identical pieces of samples for positron lifetime measurement. About  $10^6$  total counts were accumulated for each spectrum. Theoretical positron lifetime calculations were performed by using the atomic superposition (ATSUP) method proposed by Puska and Nieminen.<sup>1</sup> The electron density and the positron crystalline Coulomb potential were constructed by the non-self-consistent superposition of free atom electron density and Coulomb potential in the absence of the positron. The electron-positron enhancement factor was used in the positron lifetime calculations, which was described within the generalized gradient approximation by Barbiellini et al.<sup>2</sup> Positron lifetime calculations were performed for unrelaxed structure monovacancy defects and vacancy associates in BiOBr using  $3 \times 3 \times 2$  supercells.

**Detection of reactive oxygen species (ROS).** DPBF and NBT were used as ROS probe molecules to detect the generation of  $^1\text{O}_2$  and  $\bullet\text{O}_2^-$ , respectively. Typically, 0.01 g tested sample was added to 40 mL ethanol solution which contained 0.8 mg DPBF (for  $^1\text{O}_2$  detection) or 8 mg NBT (for  $\bullet\text{O}_2^-$  detection). Prior to illumination, the mixture was stirred in dark for 100 min to reach the adsorption-desorption equilibrium. Then the solution was exposed to visible-light irradiation under stirring by using a Xenon lamp (Bilon Co. Ltd, Shanghai, China) with a 420 nm long pass filter as the light source. At each given time interval, 2 mL suspension was sampled to determine the remaining DPBF and NBT by using a Shimadzu UV 2800 spectrophotometer. To verify the molecular oxygen involved process,  $\text{N}_2$  and  $\text{O}_2$  was pumped into the reaction system to determine the production of ROS under identical conditions. In the trapping experiments, tryptophan (10 mg), SOD (3000 unit/mL, 100  $\mu\text{L}$ ), mannitol (7.2 mg), and catalase (3000 unit/mL, 100  $\mu\text{L}$ ) was used as  $^1\text{O}_2$ ,  $\bullet\text{O}_2^-$ ,  $\bullet\text{OH}$  and  $\text{H}_2\text{O}_2$  trapping agent, respectively. All the experiments were performed under identical conditions.

**Photocatalytic organic reaction.** Diphenyl sulfide, thioanisole, 4-chlorothioanisole, 4-methoxythioanisole, 2-bromothioanisole, dimethyl sulfide, diethyl sulfide and

triphenylphosphine was selected as the substrate to evaluate the photocatalytic oxidation ability and selectivity of **BOR** samples, respectively. In a typical reaction, 50 mg tested sample was added to 10 mL acetonitrile in a Pyrex vessel. After stirring the reaction mixture for 30 min in dark, O<sub>2</sub> was purged into the Pyrex vessel to raise the initial pressure to 0.1 MPa. The reaction mixture was magnetically stirred and illuminated under visible-light (300 W Xe lamp,  $\lambda > 420$  nm, Beijing China Education Au-light Co. Ltd) irradiation at 30 °C. After reaction, the photocatalyst was separated from the reaction mixture by centrifugation, and the products were qualitatively and quantitatively analyzed by gas chromatography (GC, Agilent 7890A) equipped with a flame ionization detector (FID) and gas chromatography-mass spectrum (GC-MS, Shimadzu GCMS-QP2010).

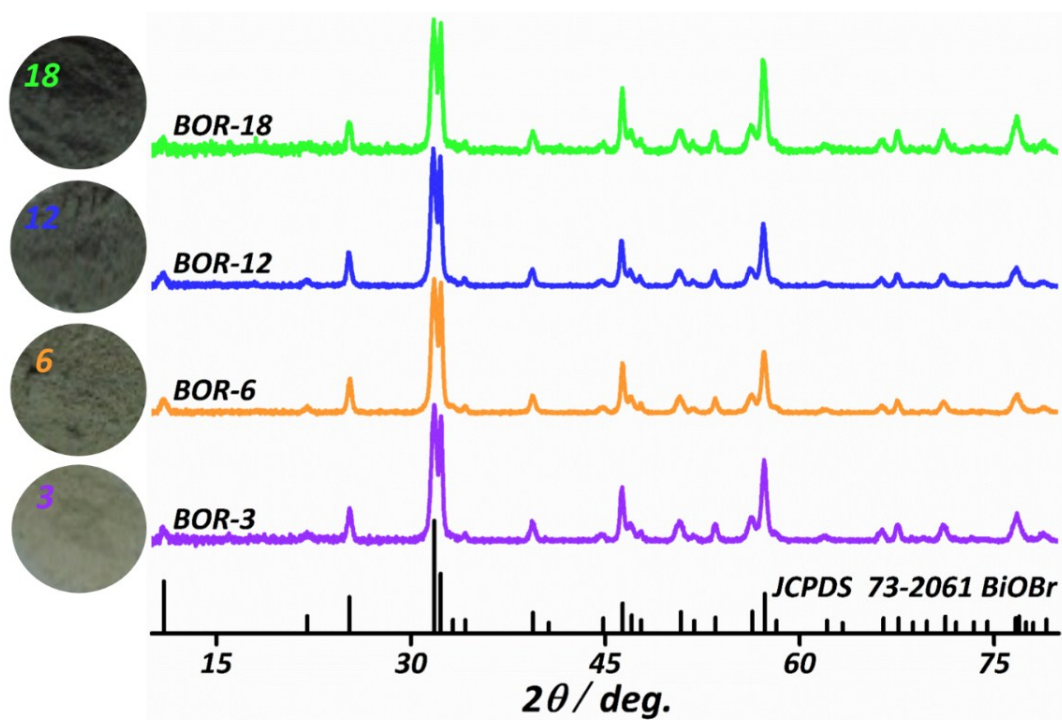


**Figure S1.** XRD patterns and photos (inset) of BiOBr products fabricated from 3 h (**BOR-3**), 6 h (**BOR-6**), 12 h (**BOR-12**) and 18 h (**BOR-18**) respectively.

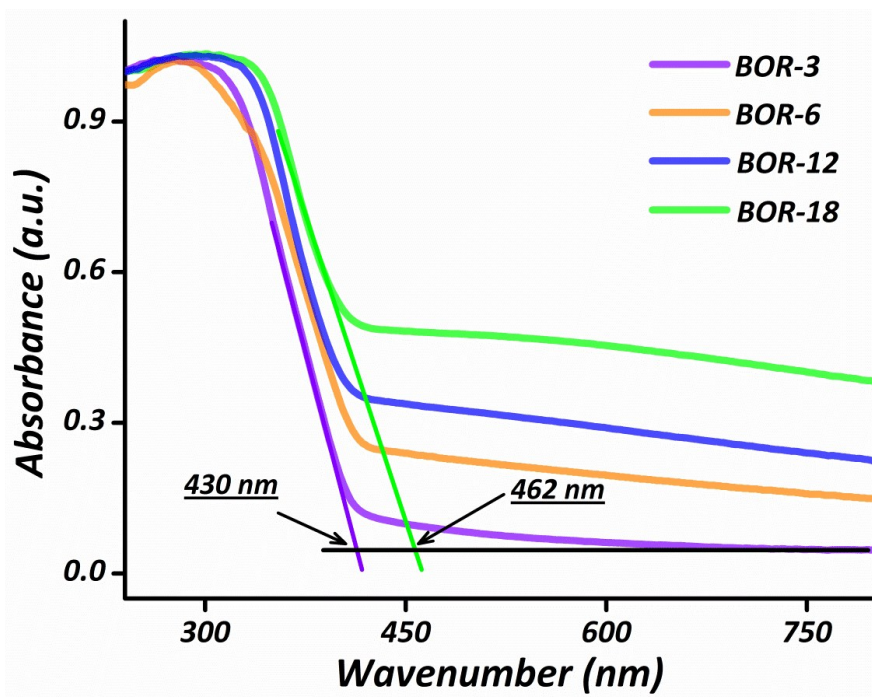
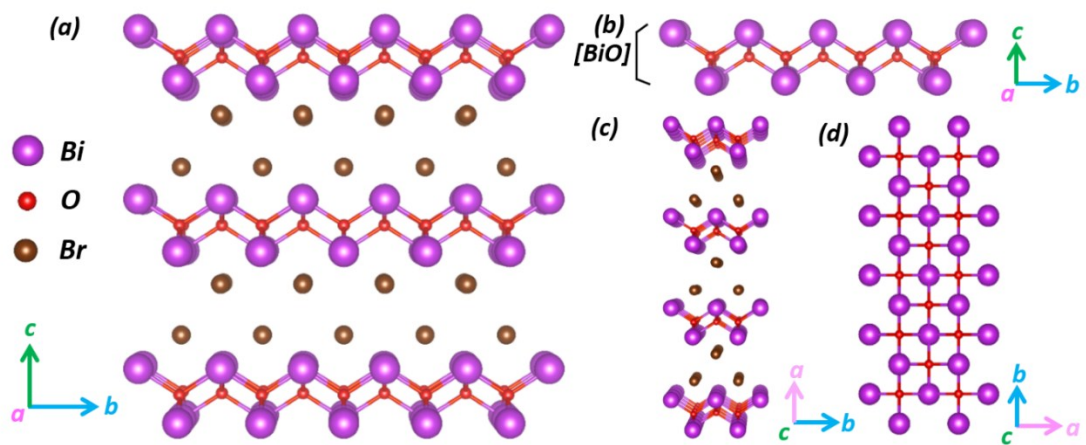
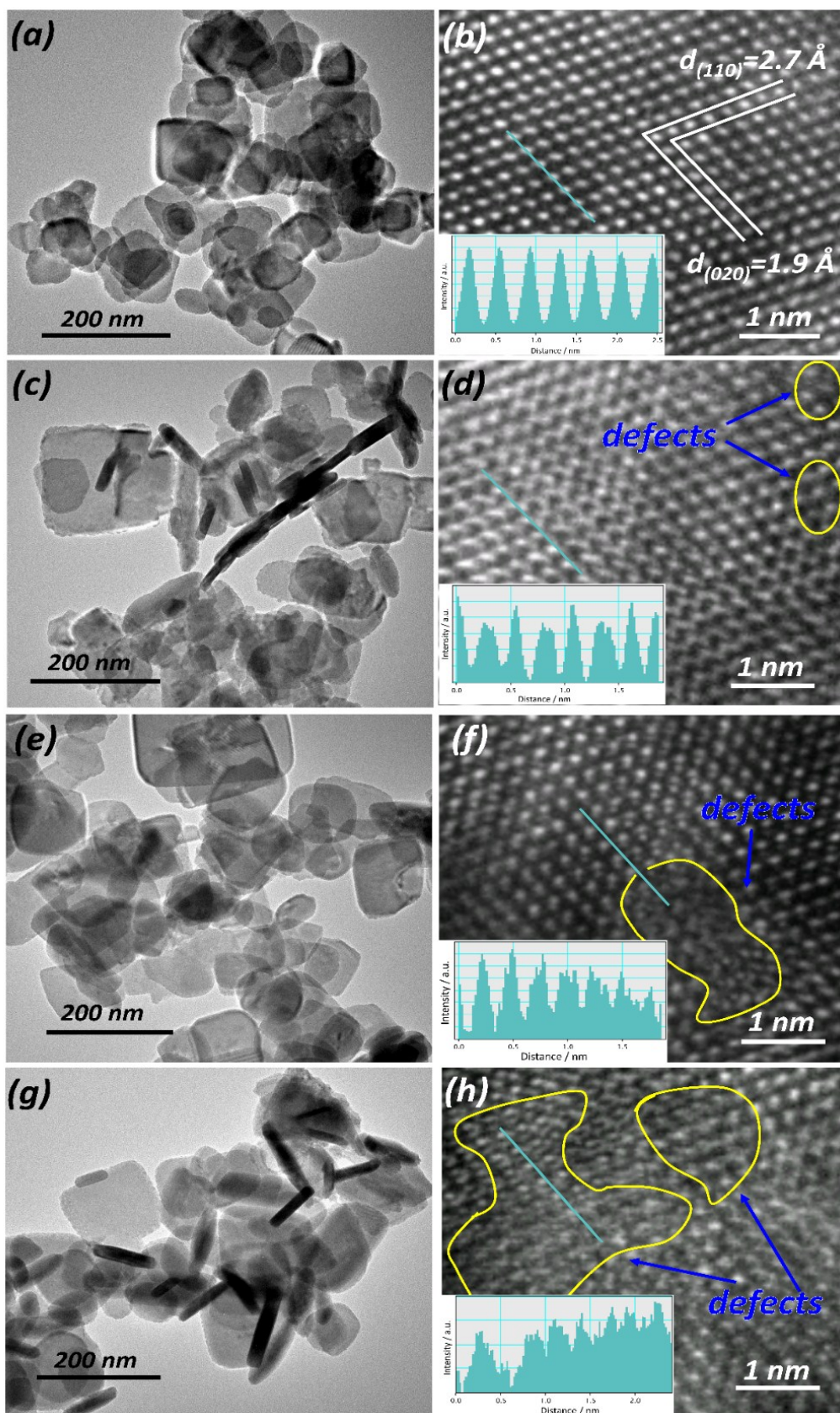


Figure S2. DRS spectra of as-synthesized BOR samples.



**Figure S3.** Schematic representation of the crystal structure of BiOBr. Three-dimensional projection. (a)  $[Bi_2O_2]^{2+}$  layers along with the  $[010]$ ,  $[001]$  and  $[100]$  direction, respectively. (b, c and d)





**Figure S4.** Transmission Electron Microscope (TEM, up) and atomic-resolution HAADF-STEM image (Inset: the corresponding intensity profile along the cyan line) of BiOBr products fabricated from 3 h (BOR-3), 6 h (BOR-6), 12 h (BOR-12) and 18 h (BOR-18).

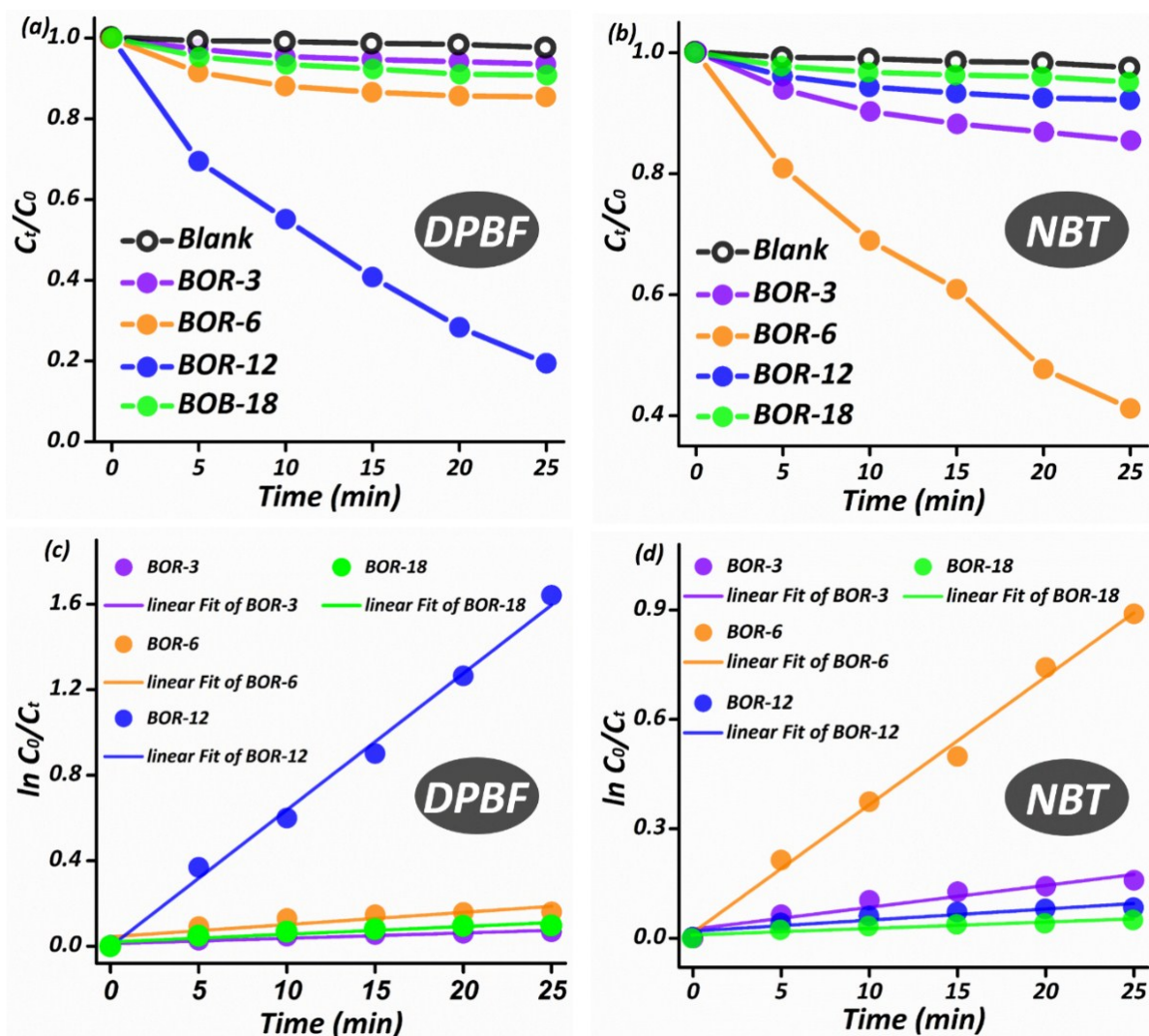


**Figure S5.** Dynamic conversion of 1,3-Diphenylisobenzofuran (DPBF) (a), nitroblue tetrazolium (NBT) (b), the pseudo-first order fitting spectrum of photochemical reaction of DPBF (c) and NBT (d) under visible light irradiation in the presence of the as-prepared **BOR** samples fabricated from 3 h (**BOR-3**), 6 h (**BOR-6**), 12 h (**BOR-12**) and 18 h (**BOR-18**) solvothermal treatments. for **BOR** samples, respectively.

The kinetics data of NBT and DPBF photochemical reaction over **BOR** samples fitted to a pseudo-first model (Figure S5c and 5d), which also illustrated the highest photoreactive rate of NBT transformation over **BOR-6** and DPBF transformation over **BOR-12**. The result also confirmed that **BOR-6** and **BOR-12** were favorable to the production of  $\bullet O_2^-$  and  $^1O_2$ , respectively.

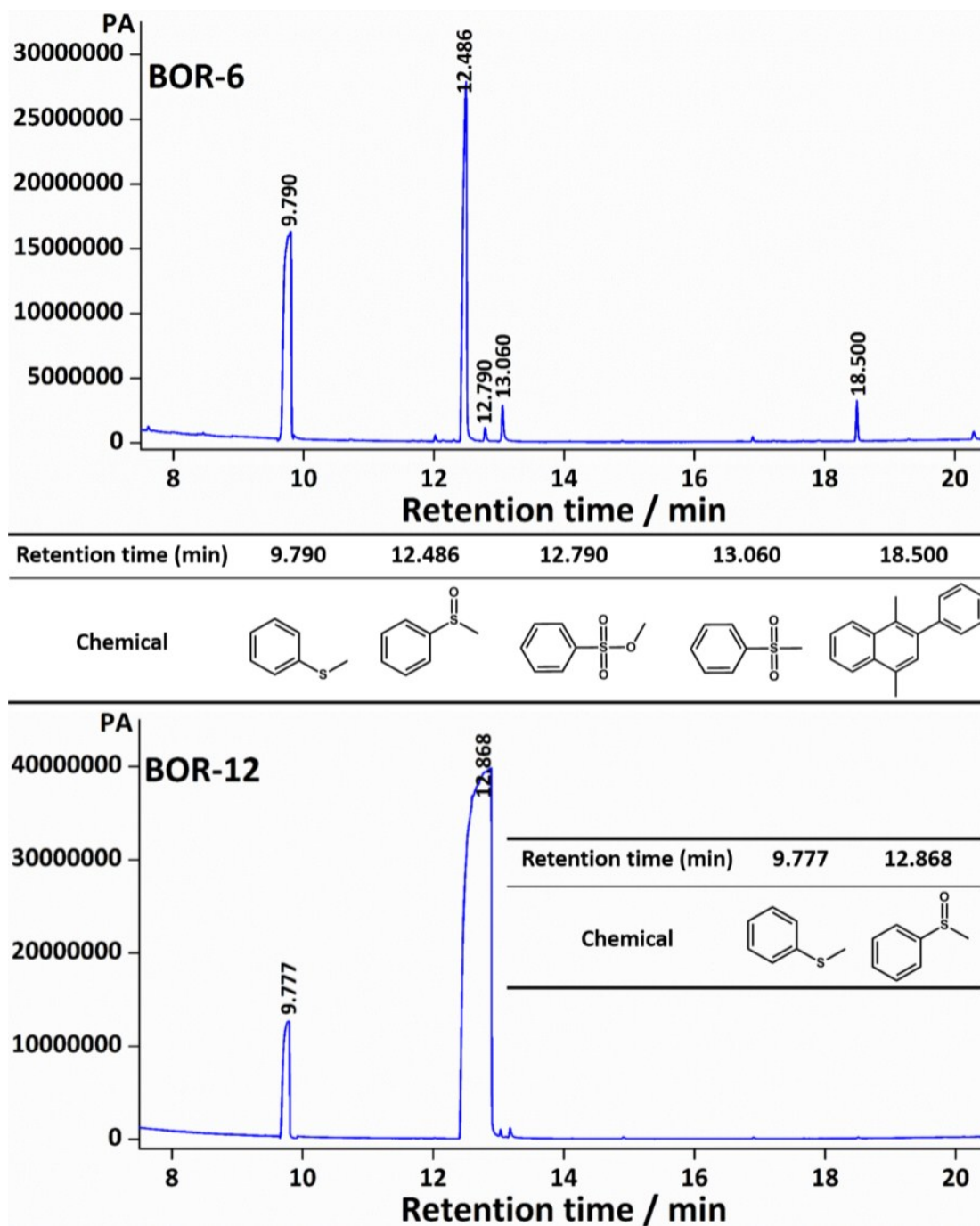


**Figure S6.** GC-FID results of photocatalytic oxidation for thioanisole over **BOR-6** and **BOR-12** under visible light irradiation.

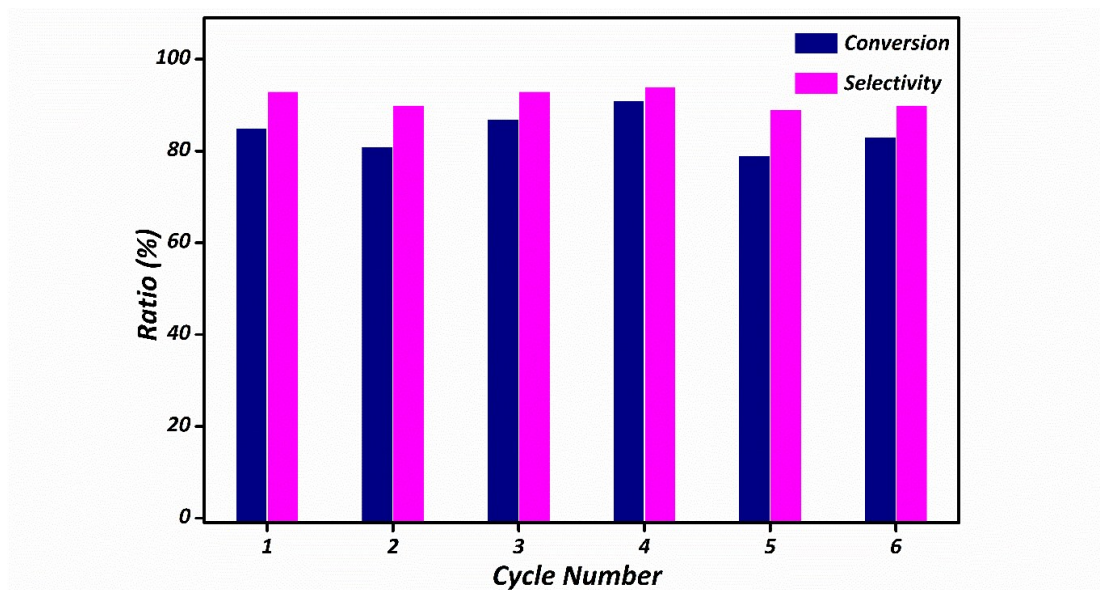


**Figure S7.** Cycling measurements of selective thioanisole oxidation with **BOR-12** samples, indicating its excellent stability and reusability.

**Figure S8.** GC-FID results for Table 3.

The results were all obtained using a split mode: for entry 1-8, the split ratio is 1/20.

Table 3, Entry 1

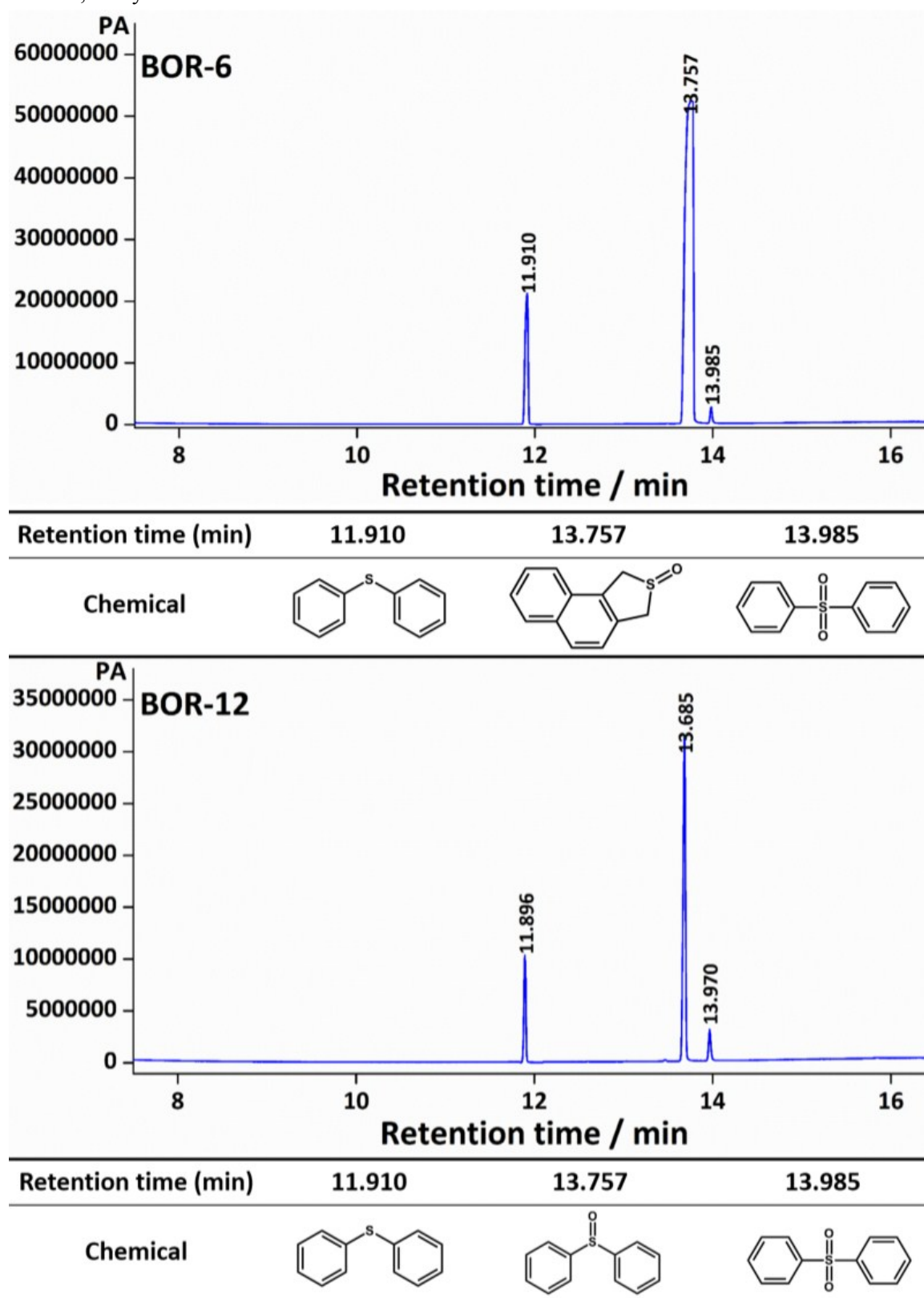


Table 3, Entry 2

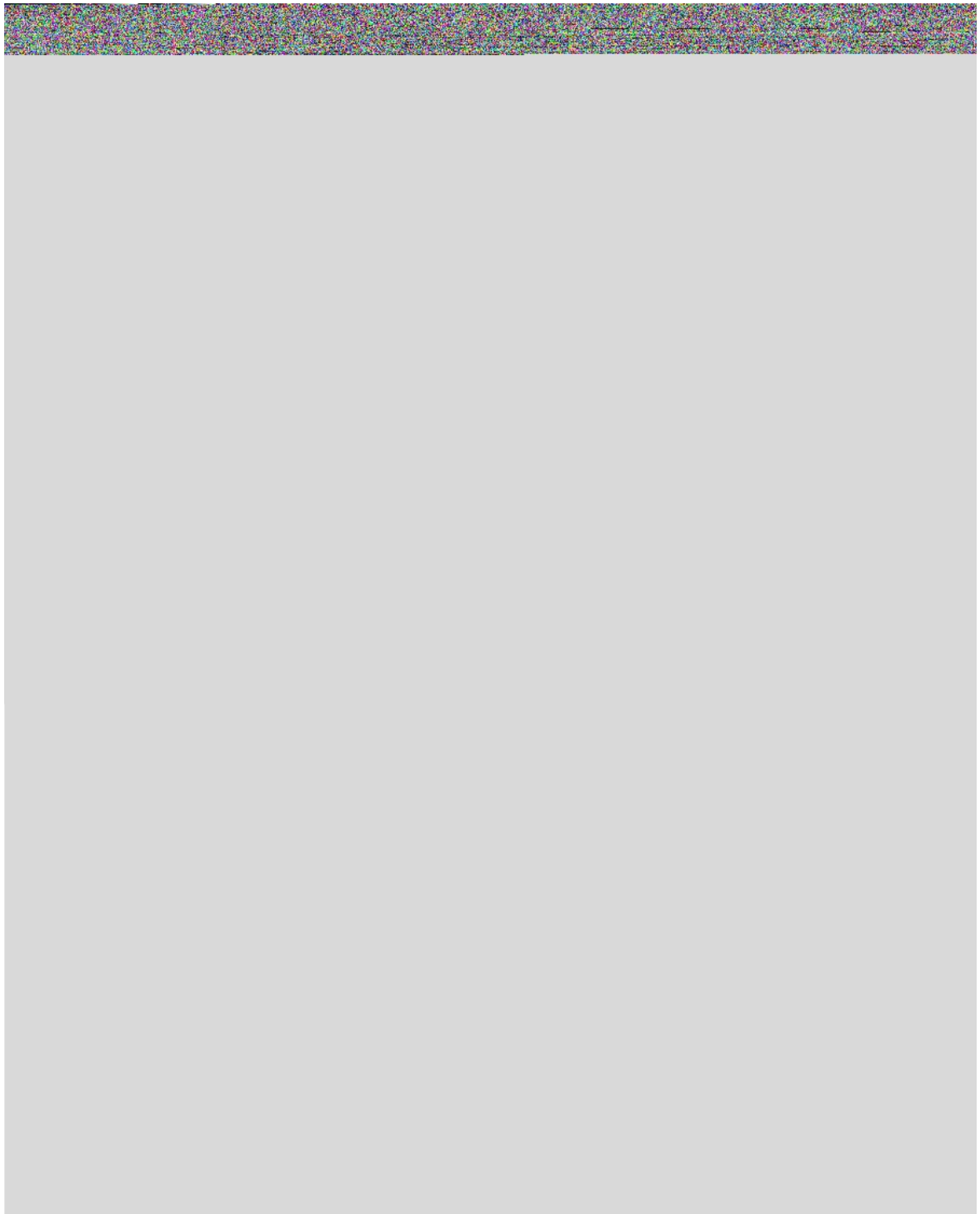
The image shows a large, solid gray rectangular area that occupies most of the page below the caption. This area is completely blank and uniform in color, suggesting it is a redaction of sensitive information or a placeholder for a table that has been obscured. The caption 'Table 3, Entry 2' is positioned at the top left of this gray area.

Table 3, Entry 3

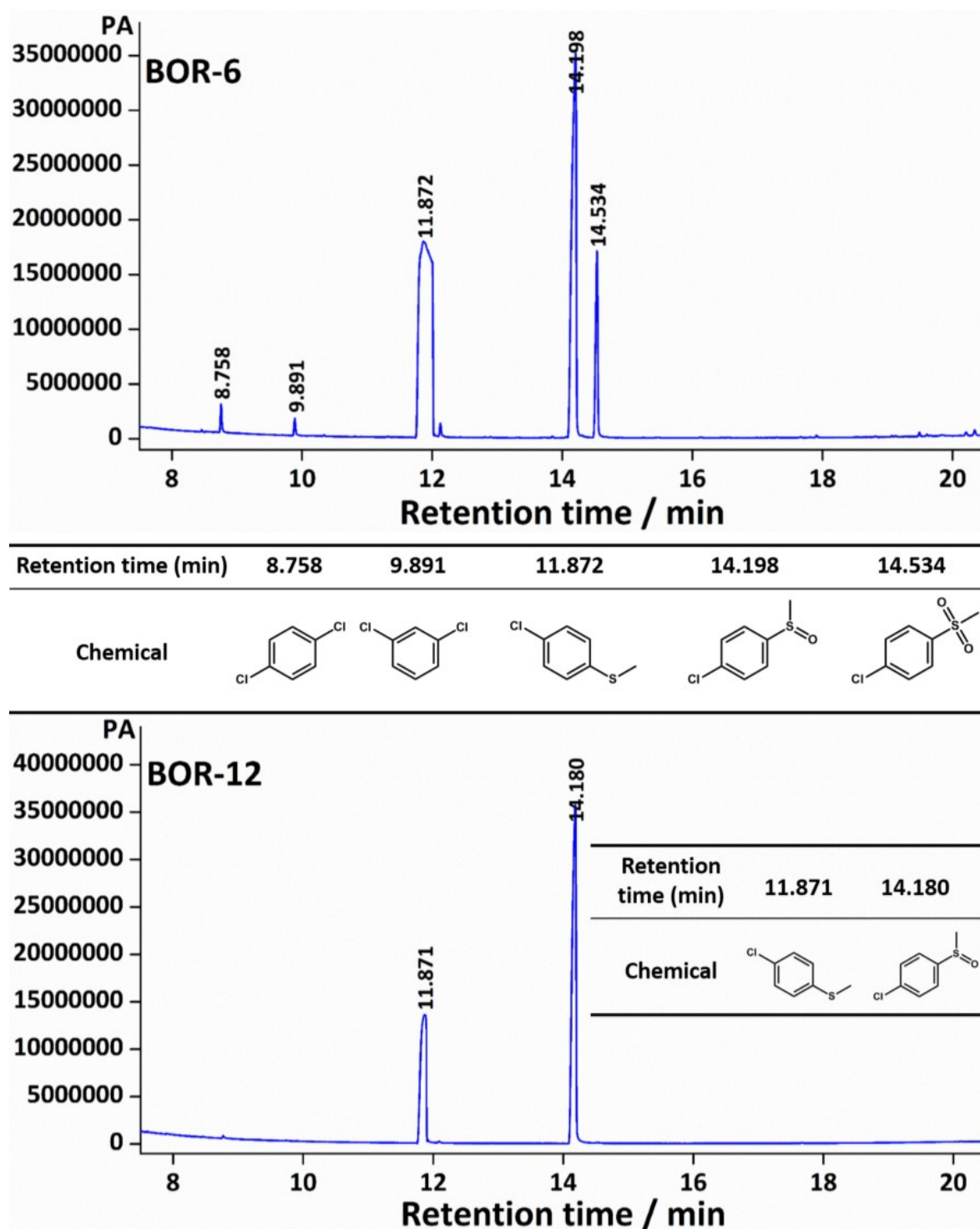


Table 3, Entry 4

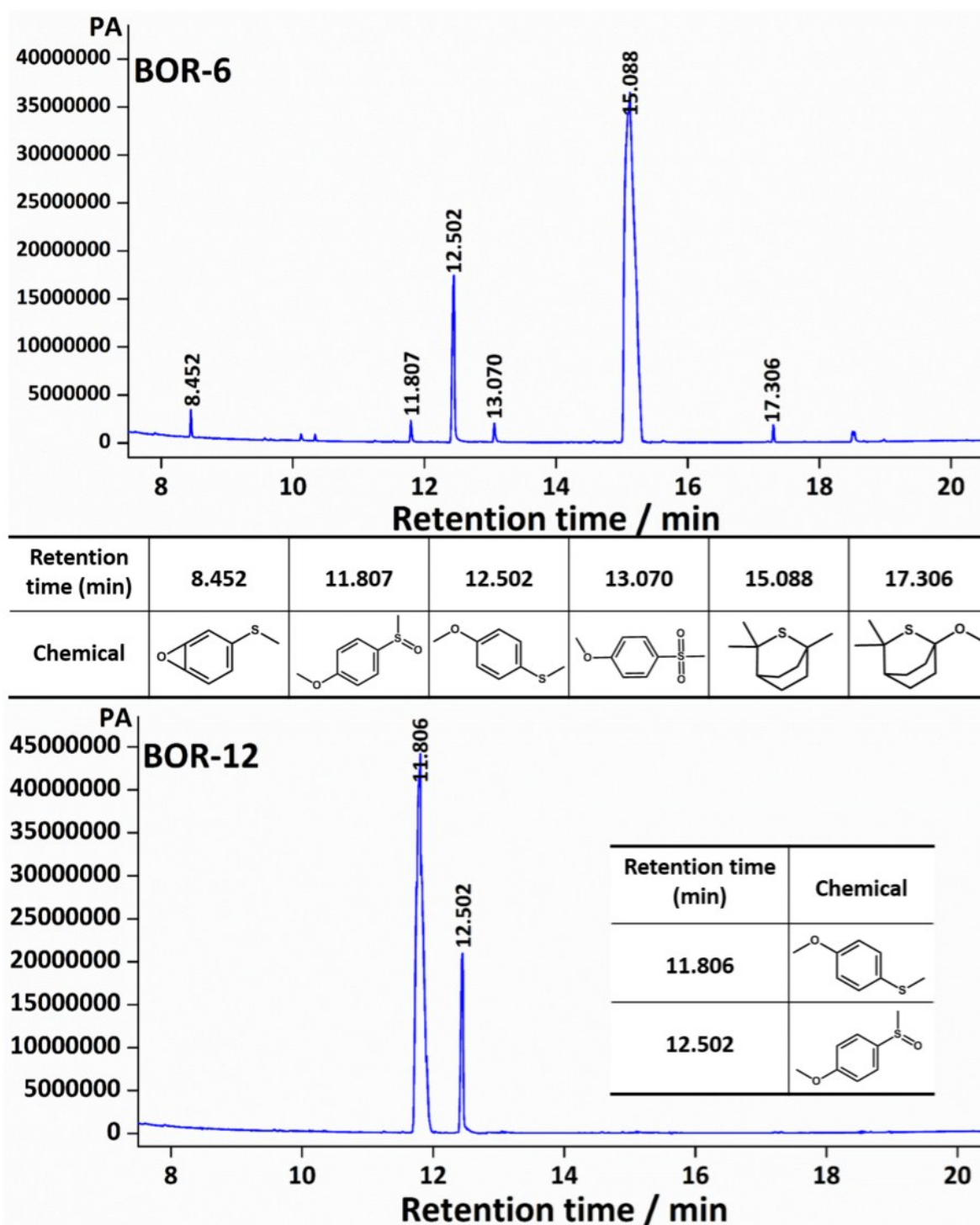




Table 3, Entry 5

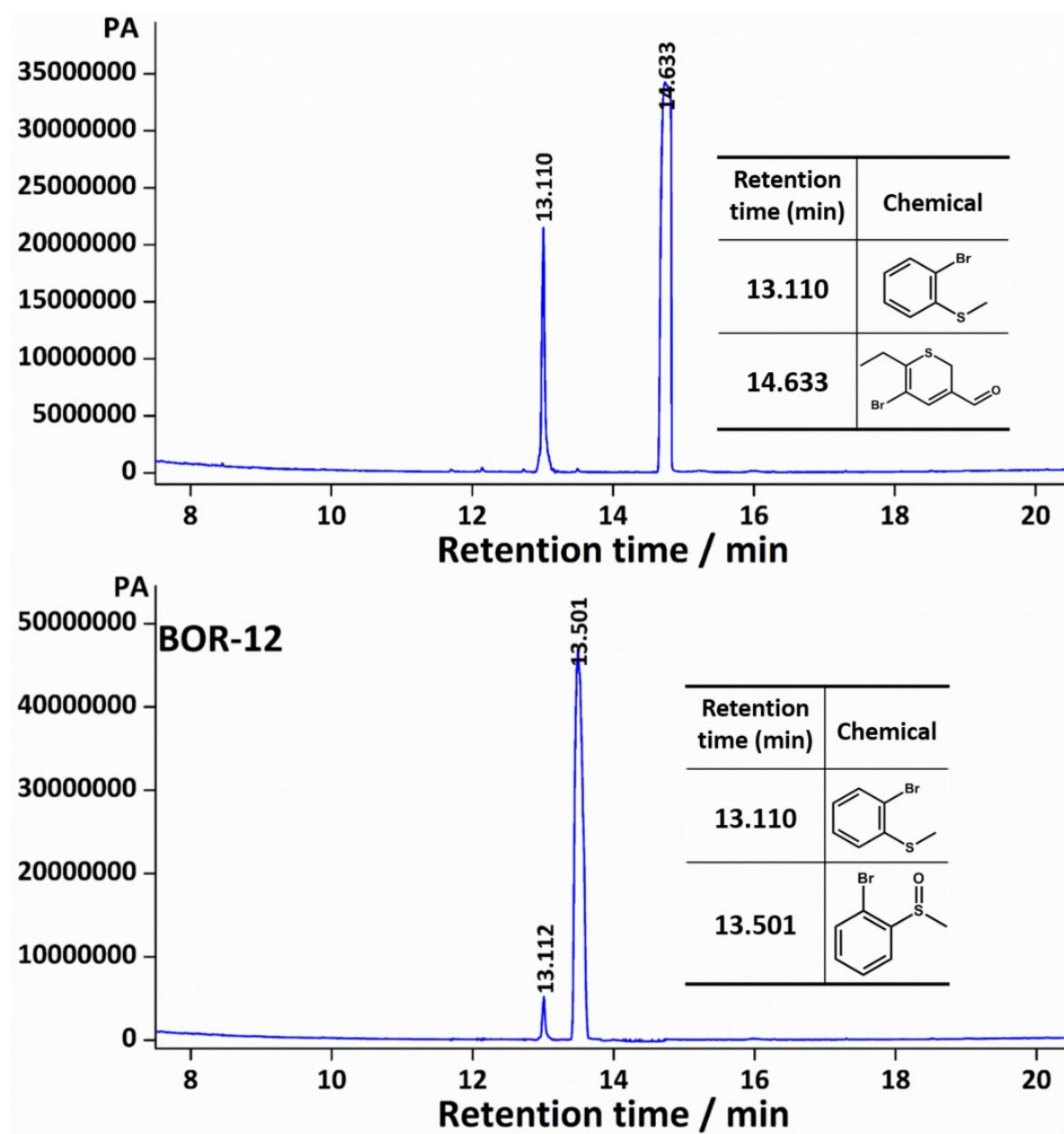


Table 3, Entry 6

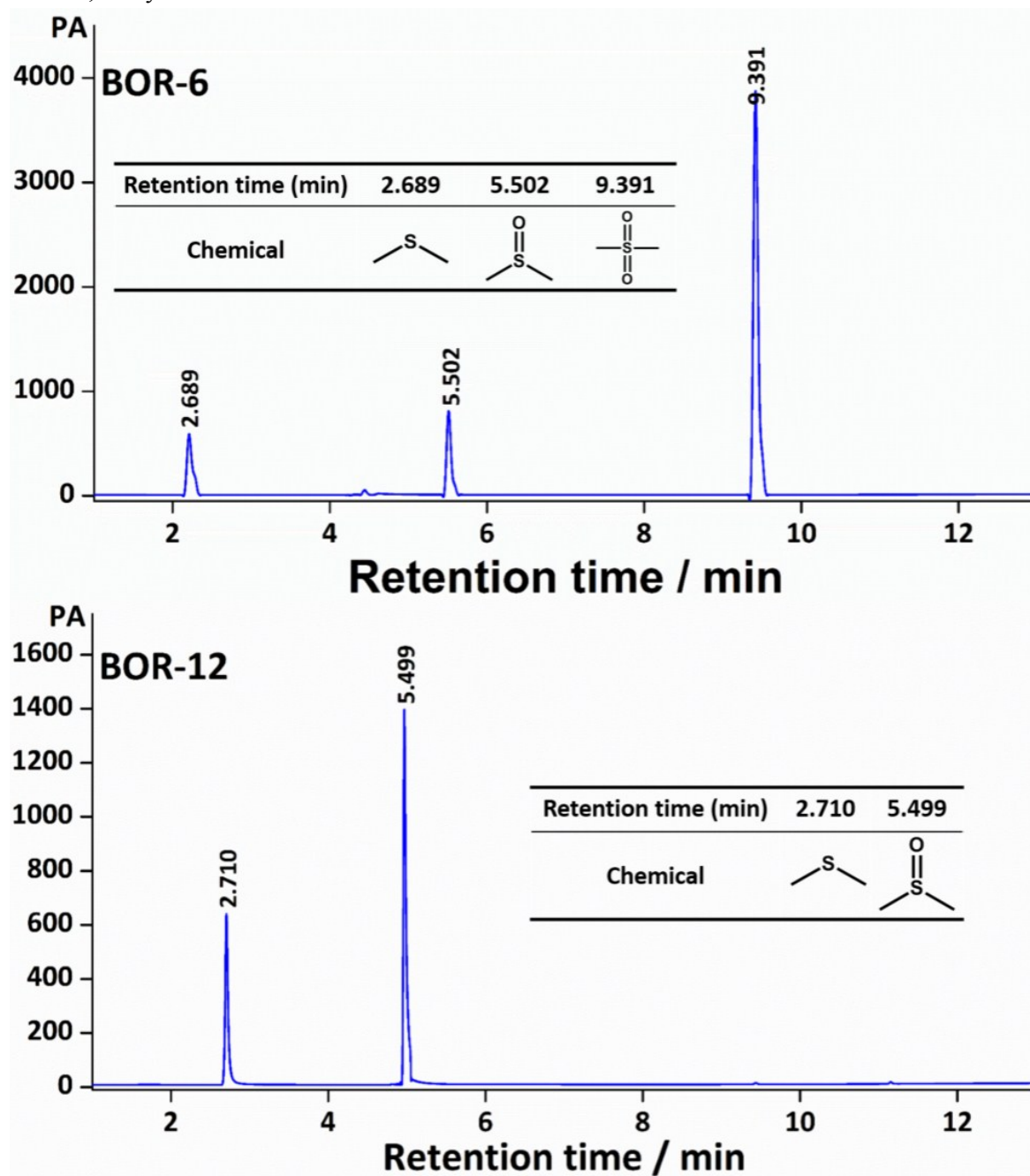
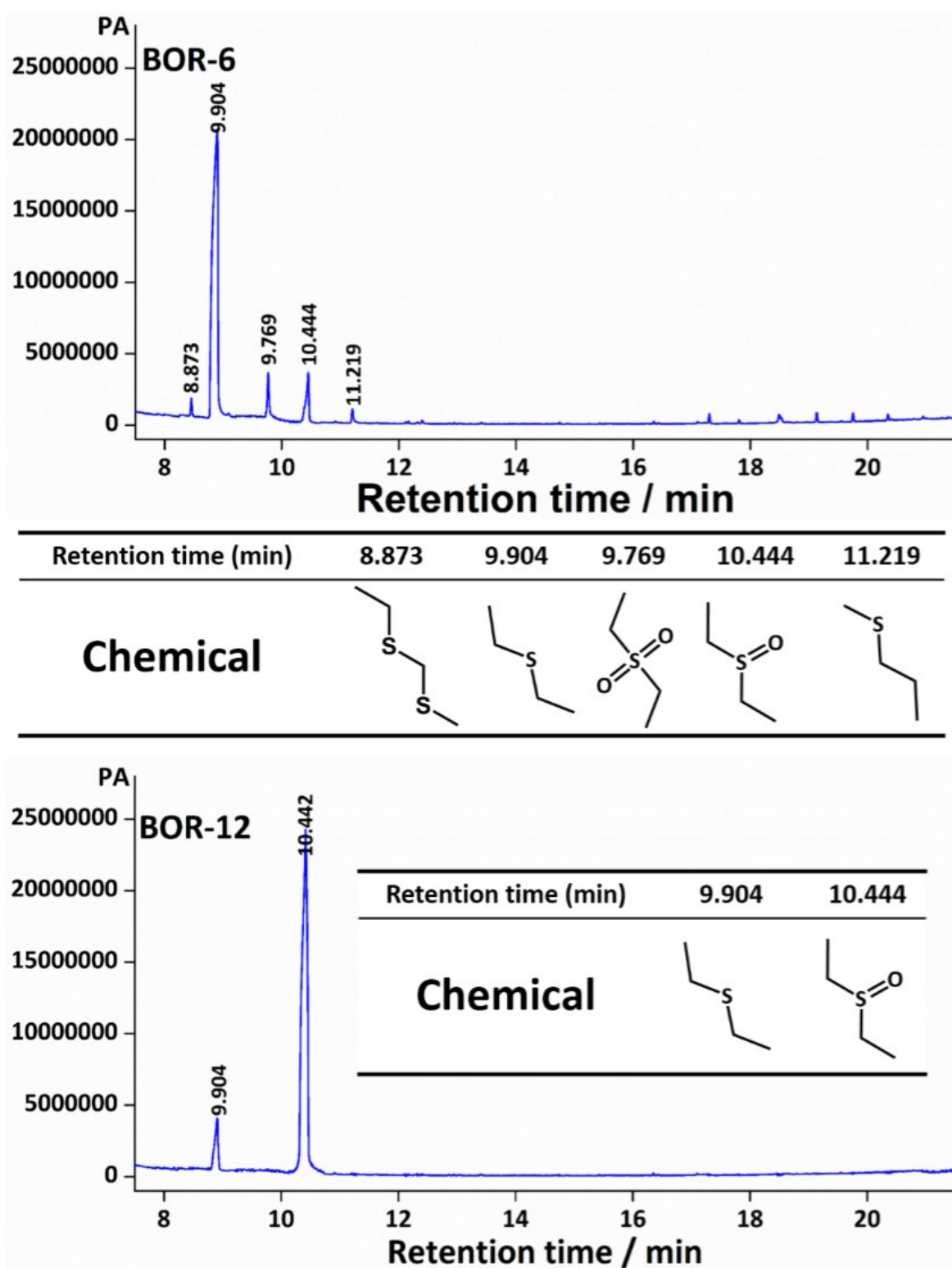
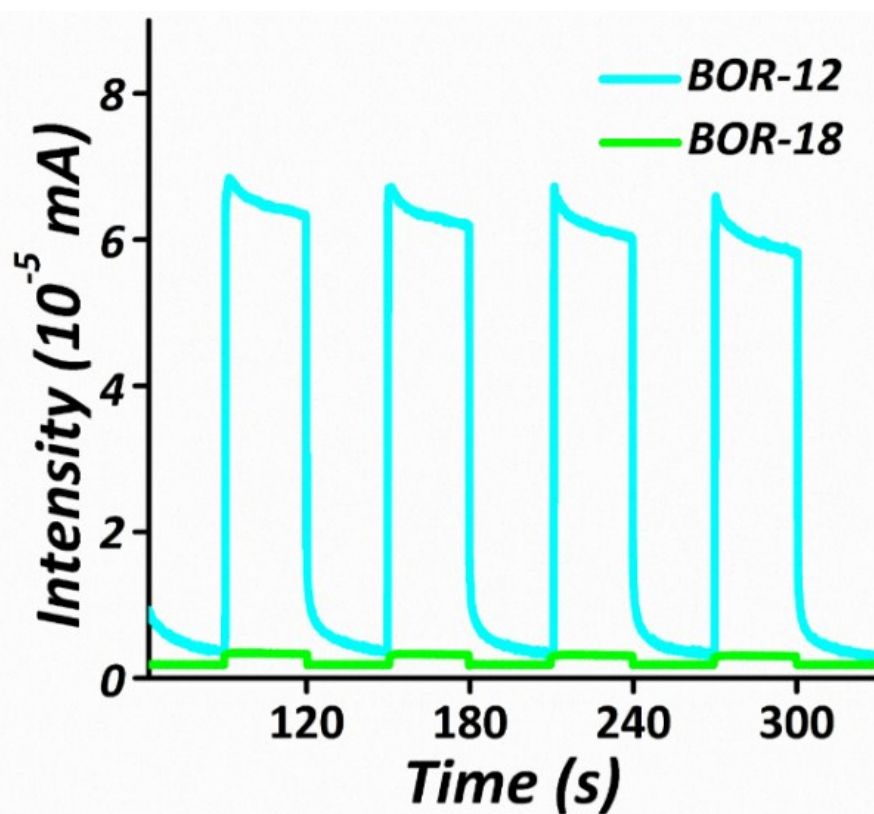


Table 3, Entry 7





**Figure S9.** Transient photocurrent responses of **BOR-12** and **BOR-18** under visible light irradiation.

**Table S1. Calculated positron lifetime (ps) values of BiOBr**

<i>defect</i>	<i>lifetime</i>	<i>defect</i>	<i>lifetime</i>	<i>defect</i>	<i>lifetime</i>
bulk	221.1	$V_{Bi}^{\bullet\bullet}V_{Bi}^{\bullet\bullet}$	245.4	$V_O^{\bullet\bullet}V_{Bi}^{\bullet\bullet}V_O^{\bullet\bullet}$	245.9
$V_{Bi}^{\bullet\bullet}$	234.2	$V_O^{\bullet\bullet}V_O^{\bullet\bullet}$	221.4	$V_{Bi}^{\bullet\bullet}V_O^{\bullet\bullet}V_{Bi}^{\bullet\bullet}$	258.4
$V_O^{\bullet\bullet}$	221.3	$V_{Br}^{\bullet}V_{Br}^{\bullet}$	285.3	$V_{Br}^{\bullet}V_{Bi}^{\bullet\bullet}V_{Br}^{\bullet}$	309.2
$V_{Br}^{\bullet}$	265.4	$V_{Bi}^{\bullet\bullet}V_O^{\bullet\bullet}$	238.9	$V_{Br}^{\bullet}V_{Bi}^{\bullet\bullet}V_O^{\bullet\bullet}$	290.0
		$V_{Bi}^{\bullet\bullet}V_{Br}^{\bullet}$	285.5		

### Reference

- (1) Puska, M. J., Nieminen, R. M., *J. Phys. F* **1983**, *13*, 333.
- (2) Barbiellini, B., Puska, M. J., Korhonen, T., Harju, A., Torsti, T., Nieminen, R. M., *Phys. Rev. B* **1996**, *53*, 16201.